# INVESTIGATION OF THE RADIATION RESISTANCE OF TRIPLE-JUNCTION a-SI:H ALLOY SOLAR CELLS IRRADIATED WITH 1.00 MeV PROTONS[1]

Kenneth R. Lord II, Michael R. Walters and James R. Woodyard
Institute for Manufacturing Research
and
Department of Electrical and Computer Engineering
Wayne State University, Detroit, MI 48202

## SUMMARY

The effect of 1.00 MeV proton irradiation on hydrogenated amorphous silicon alloy triple-junction solar cells is reported for the first time. The cells were designed for radiation resistance studies and included 0.35 $cm^2$ active areas on 1.0 by 2.0 $cm^2$ glass superstrates. Three cells were irradiated through the bottom contact at each of six fluences between 5.10E12 and 1.46E15 $cm^{-2}$. The effect of the irradiations was determined with light current-voltage measurements. Proton irradiation degraded the cell power densities from 8.0 to 98% for the fluences investigated. Annealing irradiated cells at 200 °C for two hours restored the power densities to better than 90%. The cells exhibited radiation resistances which are superior to cells reported in the literature for fluences less than 1E14 $cm^{-2}$.

## INTRODUCTION

The Thin-Film Cell Development Workshop, conducted in conjunction with the XI Space Photovoltaic Research and Technology Conference, concluded that thin-film solar cells offer the potential for high specific power density, low cost, flexible arrays, monolithic structures and high EOL performance (ref. 1). The workshop report concludes low cost is possible if thin-film solar cell technology feeds off terrestrial photovoltaic programs, and suggested that CdTe, $CuInSe_2$ and a-Si:H alloys are potential materials for thin-film cells. The workshop report stresses more research is needed in order to understand the effects of radiation with particle energies as low as 50 keV.

Engineers are considering array designs which take advantage of the high specific power densities of thin-film cells. The designs do not include cover glasses and require cells which may be deposited on ultralight materials. The arrays must provide high EOL performance for applications of ten years duration in space environments ranging from LEO through GEO. Integrated ten-year fluences for 0.10 to 200 MeV protons range between about 1E11 and 3E15 $cm^{-2}$ for these applications; ten-year fluences for 0.05 to 10 MeV electrons are between about 4E8 and 2E16 $cm^{-2}$ (ref. 1). While there are preliminary results on the radiation resistance of thin-film cells (ref. 2), a great deal more work needs to be done to provide performance data for array engineers as well as to understand the fundamental defect generation and passivation mechanisms in thin-film solar cells.

The goals of our research program are two-fold. The first is to measure and model the radiation resistance of thin-film cells to be used in various space environments. The second is to understand the

[1] Supported by TRW Engineering & Test Division and NASA Grant 3-833.

details of both proton and electron defect generation, stability and passivation. This work reports preliminary results of our investigations of 1.00 MeV proton radiation resistance of triple-tandem solar cells fabricated from a-Si:H alloys.

Our past work served as a basis for the design of experiments reported in this work (ref. 3). It has become clear that it is important to develop experimental techniques for making large numbers of measurements to provide a statistical basis for the results. There is a potential for drawing erroneous conclusions when a single measurement is made with an irradiating particle at a given energy and fluence. It is desirable to use a number of cells for each fluence, energy and irradiating particle. Three cells is the smallest number which can be used in a study which purports to have a statistical basis. The limited resources available for studies of this type are not adequate for using three cells for each fluence, energy and irradiating particle. The basis for this statement is illustrated by considering the number of cells required for an investigation of fluences in the 1E11 to 1E16 $cm^{-2}$ range and energies from 50 keV to 5.0 MeV using both protons and electrons. If three cells are used per fluence and energy measurement, and ten measurements are made per fluence and energy decade, then 3000 cells are required for each particle type. Adding control and calibration samples increases the number to about 3200 cells for each irradiating particle type. It is our experience that obtaining a total of between 10 to 100 cells for an investigation is reasonable with available resources. Other constraints involve obtaining the resources for instrumentation designed to measure and irradiate a large number of samples.

Clearly, approaches must be considered to reduce the number of cells used in investigations of the radiation resistance of solar cells which provide results with a statistical basis. The objectives of this work are two fold. The first objective is to explore the possibility of using a small number of cells in a statistical investigation based on multiple irradiation and annealing cycles. The first step in accomplishing the objective is to evaluate the effect of multiple annealing cycles on cell parameters. The next step is to study the effect of multiple cycles, including irradiations and subsequent anneals, on the cell parameters. If the original cell parameters can be demonstrated to be restored, then a small set of cells can be used in a statistical study of the radiation resistance of thin-film solar cells. The second objective is to evaluate the cell design, uniformity of the various layers and the effect of existing variations in layer thicknesses.

## EXPERIMENTAL

The support level for this work enabled us to obtain a-Si:H alloy triple-junction cells from the Thin Film Division of Solarex, Inc., for proton irradiation studies. Solarex has developed technology for producing 12 by 13 $in^2$ modules for terrestrial applications with efficiencies of about 10% under AM1.5 global illumination; the modules employ a superstrate structure (ref. 4). We were able to collaborate with Solarex on the cell design for our experiments.[2] The design criteria for the cells used for this work were developed considering the proton beam area, cell mounting, proton energy loss and electrical contacting requirements.

The area of the irradiating beam must be larger than the active area of the cells; we are able to produce a uniform proton beam 1.0 by 1.0 $cm^2$ without resorting to scanning or foil scattering techniques. The design must take into consideration the mounting of cells on the sample manipulator in the accelerator target vacuum chamber; both the chamber dimensions and the number of cells to be irradiated during a single loading must be considered. The dimensions of the chamber and sample manipulator dictated an area 1.0 by 2.0 $cm^2$ to permit mounting 23 cells on the manipulator. Twenty-three cells makes it possible to irradiate at seven fluence levels with three cells per fluence. The remaining two cells may be used for control purposes.

---

[2] We are grateful to Dr. Robert D'Aiello, Thin Film Division, Solarex, Inc., for the design and fabrication of the cells.

Investigations of irradiation-induced defect generation mechanisms requires the proton energy in the active layers of the device to be well characterized. It is desirable for the protons to lose only a small fraction of their energy in passing through either the contacts or superstrate. The thickness of the superstrate used in this work, 0.51 mm, precludes irradiating the active layers through the superstrate. TRIM calculations (ref. 5) were carried out to determine the contact thickness which would result in a negligible energy loss of a 1.00 MeV proton energy passing through the contact layers; the calculations show the contact thickness should be less than about 200 nm (nanometers).

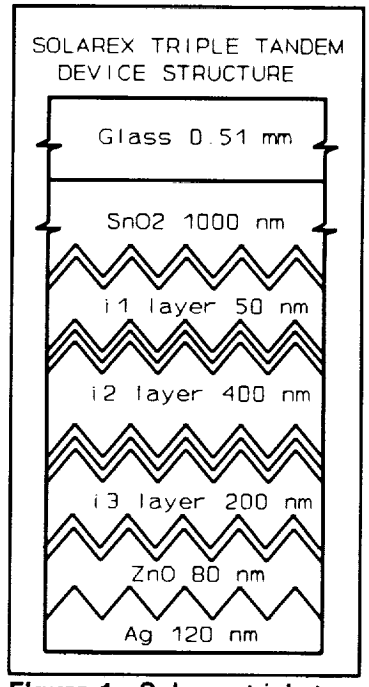


**Figure 1.** Solarex triple-tandem device structure.

The electrical contacts must be reliable under several contacting cycles and withstand temperatures of 200 °C; these requirements eliminate solder-contact methods from consideration. Laser scribing was used to isolate 0.35 by 1.0 $cm^2$ cell active areas. The active areas were contacted to two probe pads which were outside the active areas; the pads measured about 0.30 by 0.35 $cm^2$ and were defined by laser scribing during the fabrication process.

The cells were deposited on 5.0 by 5.0 $cm^2$ OCLI 0213 Ce doped glass sheets 0.51 mm thick. Ce doped OCLI 0213 glass was chosen by Solarex for the superstrate because of its superior radiation resistance; while thinner and larger area glass sheets would have been more desirable for this work, the glass sheets were selected because they were readily available. Cells measuring 1.0 by 2.0 $cm^2$ were cut by Solarex from the glass sheets by mechanical scribing following fabrication and laser scribing.

The a-Si:H alloy triple-tandem device structure used in this work has been discussed by Carlson in reference 4 and is shown in Figure 1. The layer thicknesses shown in Figure 1 were communicated by Solarex and based on processing parameters. The $SnO_2$ layer was deposited on the 0.51 mm thick glass superstrate using a chemical vapor deposition method; it is 1000 nm thick with a RMS roughness of about 30 nm; saw-tooth lines are used in Figure 1 to illustrate the $SnO_2$ surface layer roughness and its effect on the topography of the active layers of the cells. The three a-Si:H alloy junctions which make up the active layers of the cell were deposited using plasma enhanced chemical vapor deposition. The top p-i-n junction illustrated in Figure 1 has an a-Si:H intrinsic layer, i1, with an average thickness of 50 nm and a band gap of 1.72 eV. The middle p-i-n has an a-Si:H layer, i2, about 400 nm thick with a 1.72 eV band gap. The bottom p-i-n junction has an a-$Si_{1-x}Ge_x$:H layer, i3, with an average thickness of 200 nm and a band gap of 1.42 eV. The p layers of the three junctions are about 10 nm thick while the n layers range between 10 and 25 nm. The bottom contact was made by first sputter depositing an 80 nm thick ZnO layer and then a 120 nm thick Ag layer. TRIM calculations show 1.00 MeV protons lose an average of 22 keV traversing the 200 nm thick bottom contact. Hence, the cells were irradiated with 1.022 MeV protons through the bottom contact in order for protons to enter the bottom junction with an average energy of 1.00 MeV. The electronic stopping power for 1.00 MeV protons in a-Si:H is about 40 eV/nm; the nuclear stopping power is about 3.0E-2 eV/nm (ref. 5). The average energy loss of a 1.00 MeV proton in the active volume of the cell structure illustrated in Figure 1 is about 29 keV, and the stopping powers are approximately constant as the proton traverses the active layers. Most of the proton energy is deposited in the $SnO_2$ layer and glass superstrate.

The cells were illuminated using an Optical Radiation Corporation model SS1000 solar simulator equipped with a model 1522B intensity feedback controller. The solar simulator intensity was adjusted to produce the short-circuit current density, $J_{sc}$, of triple-junction cells calibrated by Solarex with their dual source AM1.5 global solar simulator (ref. 6). The spectral irradiance of our simulator was not measured; it was used with the filter provided by the manufacturer in the AM0 position. The cells were mounted on an air-cooled stage and contacted with probes. The cell temperature was monitored using the open

circuit voltage, $V_{oc}$, which was measured at the start and end of J-V measurements. The air flow was adjusted to insure the cell temperature was within one degree Celsius of the stage temperature during the measurements.

## RESULTS AND DISCUSSION

Thirty-seven a-Si:H alloy triple-tandem cells were received from Solarex for our proton radiation resistance studies. J-V measurements under illuminated conditions were used to evaluate the "as-received" cells. The cells were then annealed at 200 °C for two hours in a vacuum of about 1E-6 Torr; this anneal is referred to as anneal 1 in the discussion which follows. Following anneal 1 the J-V measurements were repeated; a fill-factor, FF, criterion of FF>0.60 was used to select cells for the investigations; 27 cells met the FF>0.60 criterion and were used in the investigations discussed in this work.

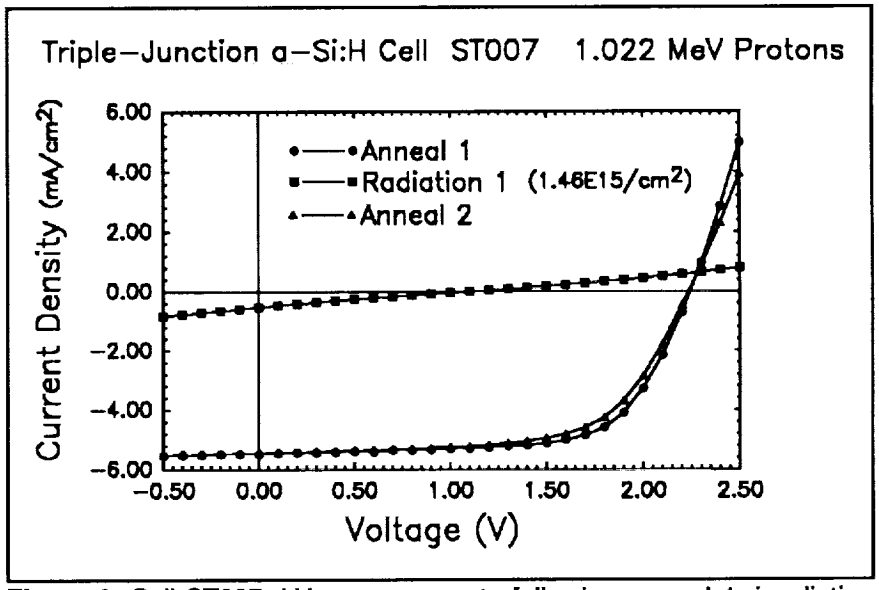


**Figure 2.** Cell ST007 J-V measurements following anneal 1, irradiation and anneal 2.

Figure 2 shows the J-V characteristics for a typical cell, ST007, following anneal 1; the J-V measurement shows the cell parameters following anneal 1 are FF=0.680, $V_{oc}$=2.24 V and $J_{sc}$=-5.46 mA/cm$^2$; the cell efficiencies are about 8.0%. The cell efficiencies are believed to be less than the 10% possible with Solarex technology for two reasons. First, the optical absorption in the OCLI 0213 glass superstrate and $SnO_2$ layer degrades the cell performance. Secondly, Solarex designed the active layers in order to spectrally match the cells to an AM0 spectrum. However, the efficiencies were measured by Solarex under an AM1.5 global spectrum. The precision of our J-V measurements was limited to about 2% because of probe contacting and solar simulator instability. The laboratory temperature ranged between 19 and 28 °C during the measurements. The effect of variations in laboratory temperature on cell parameters was investigated. Variations in FF and $J_{sc}$ were found to be insignificant at the 1% level; $V_{oc}$ values were found to vary by about 10 mV/°C and were corrected to values at 24 °C.

The effect of multiple annealing cycles on cell parameters was investigated. Six cells were investigated and the number of anneal cycles was between 10 and 12. The anneal cycle included soaking the cells at 200 °C for two hours in a vacuum of about 1E-6 Torr. Most of the cells were annealed at the same time; following each anneal cycle, the cells were removed from the anneal apparatus and the J-V characteristics measured. The cell parameters were determined from the J-V characteristics and the ratio of the standard deviation to the average cell parame-

**Table I.** The effect of annealing cycles on the ratio of the standard deviation to the average value for the FF, $V_{oc}$ and $I_{sc}$.

| Cell | FF (%) | $V_{oc}$ (%) | $I_{sc}$ (%) | Cycles (number) |
|---|---|---|---|---|
| STO24 | 1.06 | 0.47 | 1.87 | 12 |
| ST026 | 3.06 | 0.70 | 2.19 | 12 |
| ST037 | 1.81 | 0.70 | 2.20 | 10 |
| ST038 | 3.32 | 0.98 | 1.95 | 10 |
| ST039 | 1.05 | 0.68 | 2.69 | 10 |
| ST040 | 1.21 | 1.00 | 2.69 | 11 |
| Avg. | 1.81 | 0.70 | 2.20 | |

ter was calculated. The results of multiple anneal cycles on the cells are shown in Table I. The averages of the ratios for the FF, $V_{oc}$ and $I_{sc}$ range between 0.70 and 3.32%. The data show the changes in intrinsic cell parameters produced by 10 to 12 annealing cycles are less than 4% and at the level of the precision of the measurements. It is concluded the cell parameters are stable to within a few percent following multiple anneals. The finding supports the position that the effect of annealing on irradiated cells is to anneal defects produced by irradiation, instead of changing intrinsic cell parameters. Annealing studies of irradiated cells should be useful in clarifying the nature of radiation-induced defects.

Our earlier work shows device thickness plays an important role in radiation resistance (ref. 7). Three cells with FF<0.60 which had been excluded from the proton irradiation studies were analyzed using Rutherford Backscattering Spectrometry, RBS, (ref. 8). Cells with FF<0.60 were used because the radiation damage produced by 2.00 MeV $He^+$ RBS fluences is much greater than the radiation damage produced by the largest 1.022 MeV proton fluences used. RUMP simulations (ref. 9) were carried out to determine the thicknesses of the a-Si:H alloy layers, and the contact and $SnO_2$ layers. The resolution of the RBS measurements is about 20 nm for the active layers of the cells; the RUMP simulations produced active layer thicknesses with an uncertainty of about 10 nm. Figure 3 shows a spectrum for one of the cells, ST030, produced by 2.00 MeV $He^+$ RBS measurements. The RUMP simulation which yields a good fit to the data was carried out using the following layer thicknesses: 140 nm Ag; 80 nm $Zn_{0.5}O_{0.5}$; 250 nm a-$Si_{0.75}Ge_{0.25}$:H; 480 nm a-Si:H; and 1970 nm $SnO_2$. The RBS resolution is not adequate to resolve the n and p layers. The thicknesses are in good agreement with the layer thicknesses predicted by Solarex from the deposition parameters with the exception of the $SnO_2$ layer; it appears to be about twice the thickness predicted by Solarex. We are in the process of resolving the difference. RBS measurements and RUMP simulations were used to determine layer thicknesses of cells irradiated with 1.022 MeV protons; protons backscattered during 1.022 MeV irradiations were used for RBS measurements. The measurements show the variation in thickness of the active layers of the cells is less than 20%.

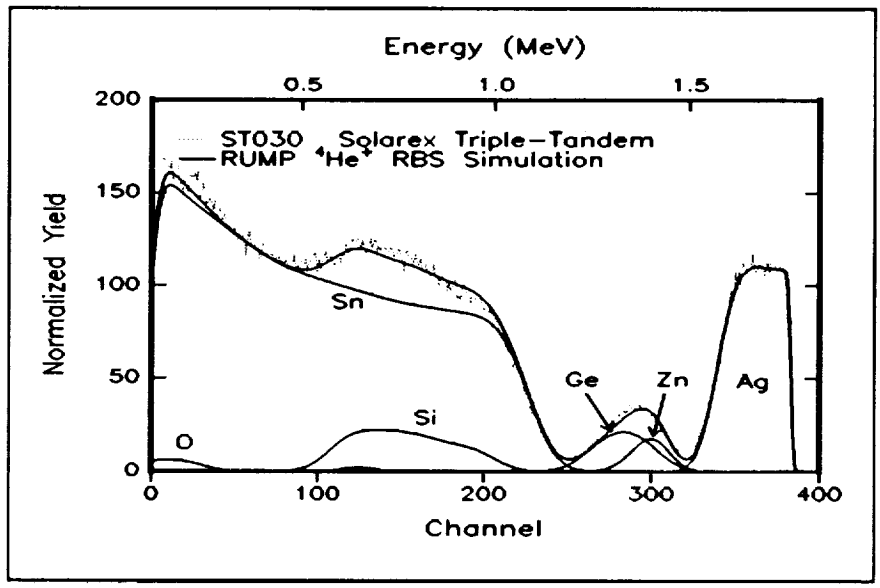


**Figure 3.** Cell ST030 2.00 MeV RBS measurements and RUMP simulation.

Twenty-one cells were mounted on a sample holder attached to a stepper-motor controlled sample manipulator in the accelerator target chamber; the chamber pressure was about 1E-6 Torr during the irradiations. Eighteen triple-tandem cells were irradiated with 1.022 MeV proton fluences. Three cells were irradiated with each of the following six fluences: 5.10E12, 1.46E13, 5.10E13, 1.46E14, 5.10E14 and 1.46E15 $cm^{-2}$. Three cells used for control purposes were mounted on the sample holder. Control cells were carried through the same steps as irradiated cells with the exception of irradiation; they were mounted between cells irradiated with the highest fluences. No radiation induced changes were measured in the control cells; this shows the beam collimation insured adjacent cells were not exposed to fluences detectable with J-V measurements. The cells were irradiated in the dark with the contact pads shorted to the sample holder. Proton beam currents between 2.5 and 50 nA were used. Cells were

visually monitored during irradiation with the aid of a video system; on one occasion a spark was observed suggesting problems with the method of shorting the cells to the sample holder. The effect of sparking on the cells is of great concern and will be investigated in our future work. Efforts will be made to improve the electrical contacting of cell contact pads to the sample holder.

Reciprocity of current and time was tested at two fluences, namely, 5.10E13 $cm^{-2}$ using currents of 10, 23 and 50 nA, and 5.10E12 $cm^{-2}$ with currents of 2.5, 5.0 and 9.0 nA. No differences in the parameters of six cells used in the reciprocity tests could be correlated with the failure of reciprocity. It is concluded that reciprocity of beam current and irradiation time holds for this work.

Following proton irradiation the cells were placed in copper ampules and transported to the device characterization laboratory. The cells were stored for 29 days in a refrigerator maintained at -10 °C and under dark conditions. The cells were stored at -10 °C because our earlier work demonstrated annealing of irradiated a-Si:H alloy cells occurs when cells are stored at 0 °C (ref. 3). Prior to measuring the J-V characteristics of a cell, the cell and copper ampule were removed from the refrigerator and placed in a desiccator, and warmed to room temperature in about 30 minutes. The cell was removed from the copper ampule, mounted in the solar simulator sample stage and probes affixed to the cell contact pads. Cell mounting and dark and light J-V measurements were completed in less than 30 minutes. Following J-V measurements, the cell was returned to the copper ampule and stored in the refrigerator. The total time elapsed during a measurement cycle, namely, the time required to remove a cell from the refrigerator, carry out the measurements, and return it to the refrigerator was less than one hour. The effect of the J-V measurement cycle on cell parameters was evaluated by repeating the measurement cycle six days later, 35 days following the irradiations. Nine cells were measured with at least one cell irradiated at each of the six fluences investigated. Results of measurements of the power density evaluated at the maximum power point on the J-V characteristic are shown in Table II. Anneal 1 data in the column labelled A1 were measured pre-irradiation; columns labelled R1 CYCLE 1 and R1 CYCLE 2 contain the data measured 29 and 35 days post-irradiation, respectively. The first measurement cycle, R1 CYCLE 1, was carried out 29 days after the irradiations with the cells stored at -10 °C; the second measurement cycle, R1 CYCLE 2, was carried out six days later with the cells stored at -10 °C following the R1 CYCLE 1 measurement. The results in Table II are presented two ways. The maximum power densities are shown for the A1, R1 CYCLE 1 and R1 CYCLE 2 measurements; the R1 CYCLE 1 and R1 CYCLE 2 measurements are normalized to A1 measurements and shown in parentheses. Table II shows a 2% change in the power density of the control cell over a 35 day period. The change in control cell power density is representative of the long-term stability in the solar simulator spectral irradiance. This shows the precision of our measurements, including stability of the simulator, is about 2% for this work. Power densities decrease with increasing fluence, as do the normalized values, but the differences between the R1 CYCLE 1 and R1 CYCLE 2 measurements are less than or equal to 2%. It is concluded the measurements show no differences in power density which can be attributed to the measurement cycle. The differences between the power densities of cells irradiated with the same fluences are about 4%; this difference is larger than the precision of the measurements.

**Table II.** Maximum and normalized power densities (shown in parentheses) measured pre-irradiation, A1, and post-irradiation, R1 CYCLE 1 and R1 CYCLE 2.

| Cell | Fluence ($cm^{-2}$) | Maximum and Normalized Power Densities ($mW/cm^2$) | | | | |
|---|---|---|---|---|---|---|
| | | A1 | R1 CYCLE 1 | | R1 CYCLE 2 | |
| ST008 | Control | 8.36 | 8.41 | (1.01) | 8.53 | (1.02) |
| ST033 | 5.10E12 | 8.44 | 7.79 | (0.92) | 7.88 | (0.93) |
| ST028 | 1.46E13 | 8.03 | 6.82 | (0.85) | 6.99 | (0.87) |
| ST021 | 5.10E13 | 8.64 | 4.76 | (0.55) | 4.92 | (0.57) |
| ST020 | 1.46E14 | 7.75 | 1.96 | (0.25) | 2.07 | (0.27) |
| ST019 | 1.46E14 | 8.06 | 1.66 | (0.21) | 1.74 | (0.22) |
| ST017 | 5.10E14 | 8.61 | 0.20 | (0.02) | 0.23 | (0.03) |
| ST009 | 1.46E15 | 8.31 | 0.03 | (0.00) | 0.04 | (0.00) |
| ST001 | 1.46E15 | 8.23 | 0.21 | (0.03) | 0.21 | (0.03) |

The results of 1.022 MeV proton irradiations on a-Si:H alloy triple-tandem cells are shown in Figure 2 and Table III. Figure 2 shows the J-V characteristics for one of the cells, ST007, which was irradiated to a fluence of 1.46E15 $cm^{-2}$. Following irradiation the cell parameters are: FF=0.227; $V_{oc}$=1.10 V; $J_{sc}$=-0.53 $mA/cm^2$;and $P_{max}$=0.13 $mW/cm^2$. The values correspond to degradation in normalized cell parameters to: FF=33%; $V_{oc}$=49%; $J_{sc}$=10%; and $P_{max}$=1.6%. Annealing cell ST007 at 200 °C for two hours resulted in the recovery of the J-V characteristic as shown in Figure 2. The normalized cell parameters recovered to the following percentages of the pre-irradiation values: FF=94%; $V_{oc}$=99%; $J_{sc}$=100%; and $P_{max}$=93%. The J-V characteristic observed for cell ST007 is characteristic of the other irradiated cells with the exception that there is less degradation and better recovery for lower fluences. Table III shows the variation in the average maximum and normalized power densities. The power densities were measured at the maximum power point and the average power densities are for three cells irradiated to the fluences indicated. The average power densities in column A1 were measured on cells annealed at 200 °C for two hours prior to proton irradiation. Column R1 shows the average power densities measured 29 days after irradiation with the cells stored in the dark at -10 °C. Column (R1/A1) contains the average post-irradiation power densities normalized to the A1 values. The cells were annealed at 200 °C for two hours following R1 measurements. The average power densities under these conditions are in column A2; the A2 power densities normalized to the A1 values are shown in column (A2/A1). Table III shows 1.022 MeV protons degrade the normalized average power density to 0.92 at the lowest fluence used in this work, namely, 5.10E12 $cm^{-2}$. Increasing the fluence to 1.46E15 $cm^{-2}$ degrades the normalized average power density to about 0.02. Annealing the cells restored the average power densities to the pre-irradiation values for fluences less than and equal to 5.10E13 $cm^{-2}$. For fluences above this value, a two-hour anneal at 200 °C restores the average power densities to within 90% of the pre-irradiation values. We expect that annealing for longer times will restore the average power densities for these higher fluences.

**Table III.** Maximum and normalized average power densities under pre-irradiation, A1, post-irradiation, R1, and post-irradiation annealed, A2, conditions.

| Fluence ($cm^{-2}$) | Maximum and Normalized Average Power Densities ($mW/cm^2$) | | | | |
|---|---|---|---|---|---|
| | A1 | R1 | (R1/A1) | A2 | (A2/A1) |
| Control | 8.18 | 8.26 | (1.01) | 8.32 | (1.02) |
| 5.10E12 | 8.26 | 7.60 | (0.92) | 8.42 | (1.02) |
| 1.46E13 | 8.27 | 6.74 | (0.82) | 8.52 | (1.03) |
| 5.10E13 | 8.04 | 4.24 | (0.53) | 8.20 | (1.02) |
| 1.46E14 | 8.16 | 1.84 | (0.23) | 7.66 | (0.94) |
| 5.10E14 | 8.31 | 0.39 | (0.05) | 8.10 | (0.98) |
| 1.46E15 | 8.31 | 0.13 | (0.02) | 7.55 | (0.91) |

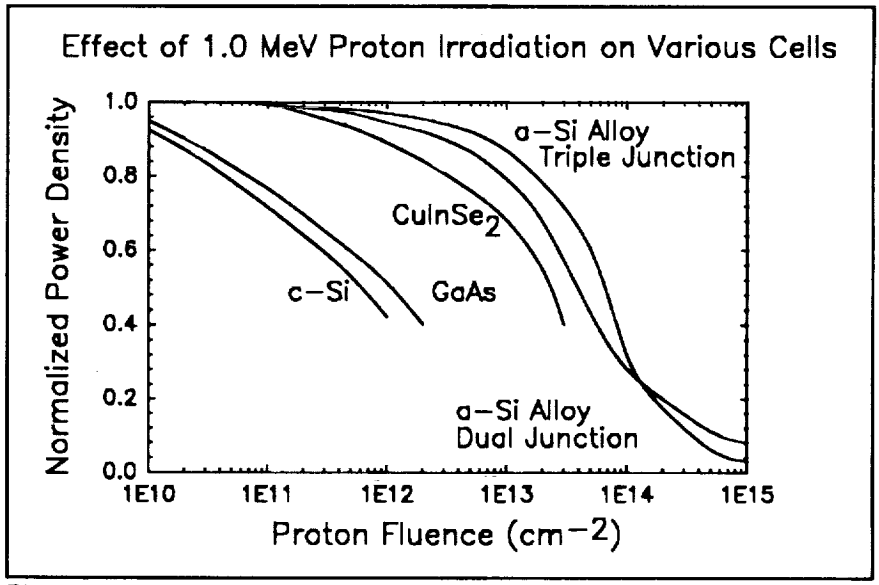


**Figure 4.** Normalized cell power for crystalline Si and GaAs, $CuInSe_2$ and a-Si:H solar cells irradiated with 1.00 MeV protons.

The normalized average power densities for the triple-tandem a-Si:H alloy solar cells following irradiation are compared to different types of solar cells in Figure 4. Smooth curves are plotted through the normalized power densities measured following irradiation of the cells with

various proton fluences. One MeV proton irradiation of crystalline Si and GaAs cells (ref. 10), and $CuInSe_2$ cells (ref. 11) are shown along with dual-junction a-Si:H alloy cells (ref. 12). Data for 1.00 MeV proton irradiation of InP have not been published; 10 MeV proton data for fluences below 5E12 $cm^{-2}$ have been published (ref. 13); the data are not shown in Figure 4 but would fall between the dual-junction tandem a-Si:H alloy and $CuInSe_2$ curves. The stopping power of 10 MeV protons in InP is less at 1.00 MeV. InP data resulting from 1.00 MeV proton irradiation will be shifted to lower normalized cell powers. Figure 4 shows triple-junction a-Si:H alloy cells have a 1.00 MeV proton radiation resistance superior to other cells for fluences less than about 1E14 $cm^{-2}$; dual junction a-Si:H alloy cells have better radiation resistance for fluences above 1E14 $cm^{-2}$.

The degradation in the average value of parameters for cells irradiated with 1.00 MeV protons is shown in Figure 5. The percent of the pre-irradiation average values of FF, $V_{oc}$ and $J_{sc}$ are shown versus fluence; the average values of the cell parameters were determined using the data from three cells irradiated to the same fluence. The decrease in average cell power density is dominated by FF for fluences up to about 5E13 $cm^{-2}$; above this fluence, $J_{sc}$ dominates the degradation in the power density.

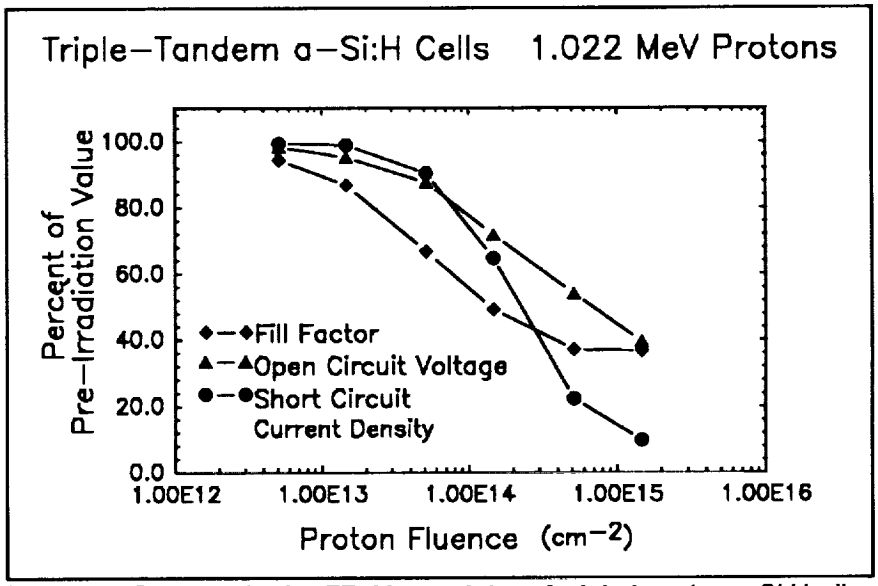


**Figure 5.** Changes in the FF, $V_{oc}$ and $J_{sc}$ of triple-junction a-Si:H alloy solar cells produced by 1.022 MeV proton irradiation.

Figure 6 shows the manner in which FF varied for all irradiated cells along with the average values; the figure also shows FF following one anneal of each cell at 200 °C for two hours. The scatter in post-irradiation FF at each fluence and the corresponding FF following annealing is within the scatter of the pre-irradiation values except for cell ST020 which was irradiated with a fluence of 1.46E14 $cm^{-2}$; the reason for this is not understood. With the exception of cell ST020, cells irradiated with fluences less than 5.10E14$cm^{-2}$ are restored to within 4% of the pre-irradiation FF values with annealing; cells irradiated with fluences greater than or equal to 5.10E14$cm^{-2}$ annealed within 7% of pre-irradi-

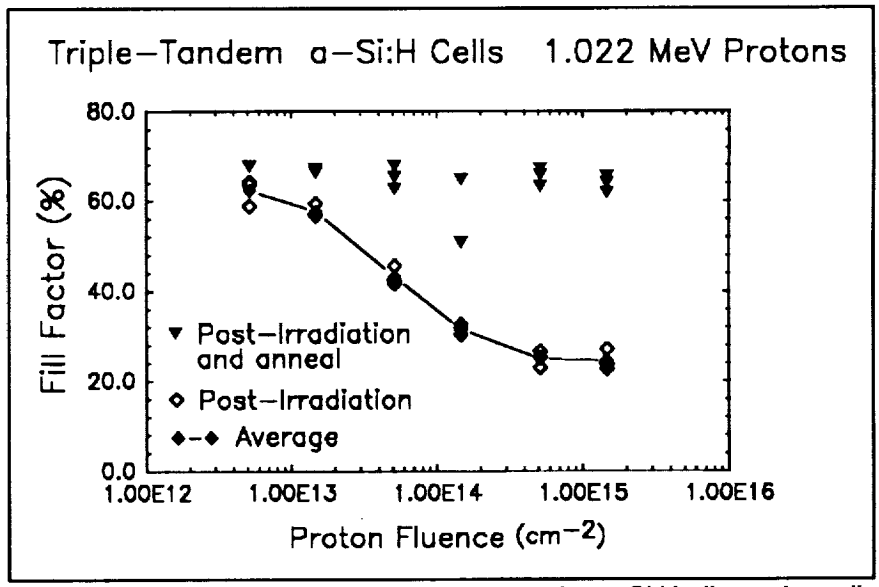


**Figure 6.** Percent change in FF of triple-junction a-Si:H alloy solar cells following 1.022 MeV proton irradiation and annealing.

ation FF values. Cell ST020 has an annealed post-irradiation FF value which differs from the pre-irradiation value by 20%.

The behavior of $V_{oc}$ with irradiation and post-irradiation annealing is shown in Figure 7. $V_{oc}$ shows scatter at each fluence following irradiation which exceeds the scatter both in the pre-irradiation and the annealed post-irradiation values. With the exception of cell ST020, annealed post-irradiation $V_{oc}$ values are within 3% of the pre-irradiation values. Cell ST020 has an annealed post-irradiation which is 5% less than the pre-irradiation $V_{oc}$. Figure 7 shows the lowest post-irradiation value of $V_{oc}$ was measured on cell ST009 which was irradiated to a fluence of 1.46E15 $cm^{-2}$. Sparking was observed during irradiation of cell ST009. The role of sparking on the post-irradiation $V_{oc}$ values and the scatter in $V_{oc}$ values of cells irradiated to the same fluence will be the subject of future investigations.

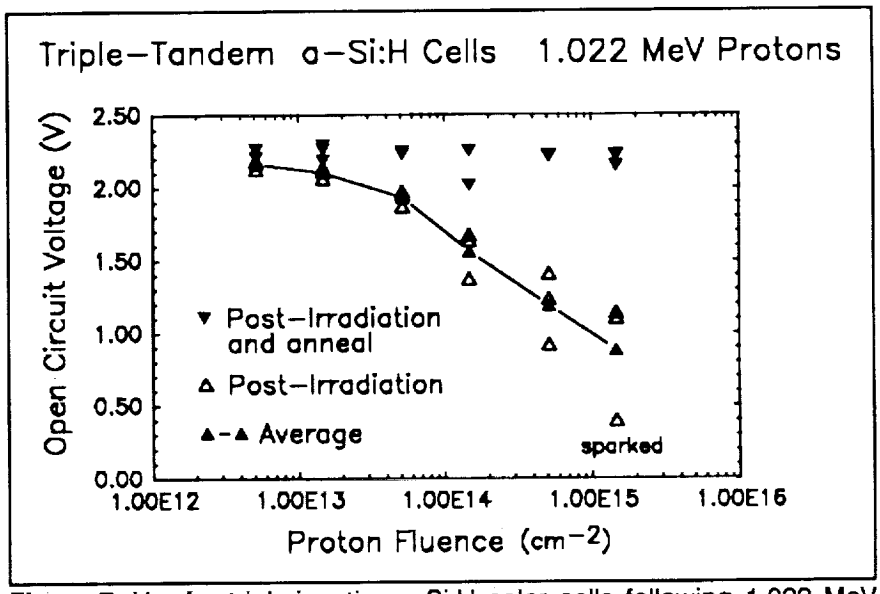


**Figure 7.** $V_{oc}$ for triple-junction a-Si:H solar cells following 1.022 MeV proton irradiation and annealing.

The correlation of scatter in $V_{oc}$ with active layer thickness was explored. RBS measurements and RUMP simulations show 14 cells have active layer thicknesses ranging between 680 and 760 nm. Four cells had active layer thicknesses ranging between 620 and 630 nm. $V_{oc}$ differences between cells of the same thickness are about the same as the cells different thicknesses. We are unable to correlate the scatter in $V_{oc}$ with cell active layer thickness.

The effect of 1.022 MeV proton irradiation on $J_{sc}$ is shown in Figure 8. The scatter in the post-irradiation values exceeds the scatter in both the pre-irradiation and annealed post-irradiation values of $J_{sc}$; the annealed post-irradiation values recovered to within 2% of the pre-irradiation values. The exception is cell ST009 which annealed to within 8% of the pre-irradiation value. The active layer thickness appears to contribute to the

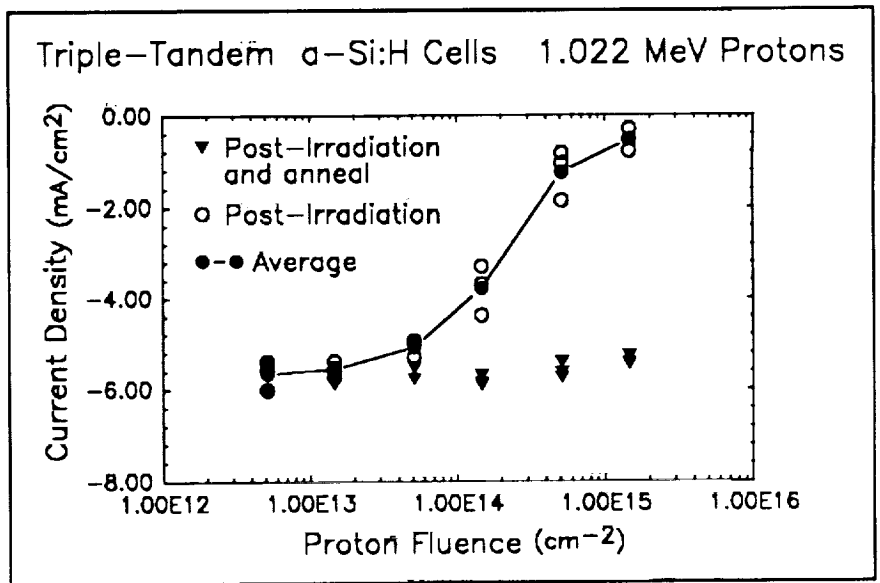


**Figure 8.** $J_{sc}$ for triple-junction a-Si:H alloy solar cells following 1.022 MeV proton irradiation and annealing.

scatter in $J_{sc}$. Cells irradiated to the same fluence with thinner active layers exhibited less degradation in $J_{sc}$ than the thicker cells.

## CONCLUSIONS

Investigations of twenty-seven triple-junction a-Si:H alloy cells for use in radiation resistance studies show the cells are stable when annealed for up to 12 cycles. The average cell power degrades from a pre-irradiation value of 8.18 to 0.13 mW/cm$^2$ following irradiation with a 1.022 MeV proton fluence of 1.46E15 cm$^2$. Reciprocity between irradiating beam current and time appears to hold for these studies. The cells have a 1.00 MeV proton radiation resistance which is superior to the other cells for fluences less than about 1E14 cm$^{-2}$; dual junction a-Si:H alloy cells have better radiation resistance for fluences above 1E14 cm$^{-2}$. A two-hour 200 °C anneal restores the power to better than 90% of the pre-irradiation value. If the two cells which produced anomalous results are eliminated from the averages, the power density recovers at the 98% level with annealing at 200 °C for two hours. Power density measurements on irradiated cells show no differences which can be attributed to the measurement cycle itself. Variations in $V_{oc}$ at the 20% and $J_{sc}$ at the 10% level were observed for cells irradiated with the same fluence. While some of the variations in $J_{sc}$ correlate with the differences in cell active layer thickness, the variations in $V_{oc}$ cannot be correlated to cell thickness. The source of the variations will be the subject of future studies. RBS measurements and RUMP simulations show the active layer thickness of the cells ranges between 620 and 760 nm; the thicknesses are within 15% of the values determined from the deposition parameters. There is a discrepancy in the $SnO_2$ layer thickness; the processing parameters suggest the layer is 1000 nm thick while RBS measurements indicate a thickness of 2000 nm. The discrepancy will be explored using other measurement techniques. The cell design developed by Solarex appears to be excellent for radiation resistance research. More research is required to determine if a set of about 25 cells can be used in radiation resistance studies employing multiple irradiation and annealing cycles. The development of experimental techniques will be continued in order to accomplish our goal of reproducing all measurements at the 1% percent level.

## REFERENCES


1. James R. Woodyard, Eleventh Space Photovoltaic Research and Technology Conference-1991, NASA Conference Publication 3121, 1991, p. 48-1.
2. James R. Woodyard and Geoffrey A. Landis, Solar Cells **31**, 1991, p. 297
3. Salman Abdulaziz, J. Scott Payson, Yang Li and James R. Woodyard, 21st IEEE Photovoltaic Specialists Conference Proceedings, 1990, p. 1510.
4. D.E. Carlson, 22st IEEE Photovoltaic Specialists Conference Proceedings, 1991, p. 1207.
5. J.F. Ziegler and W. K. Chu, IBM Report RC 4288, 1973.
6. M. S. Bennett and R. Podlesny, 21st IEEE Photovoltaic Specialists Conference Proceedings, 1990, p. 1438.
7. James R. Woodyard, Amorphous Silicon Technology-1992, Materials Research Society Symposium Proceedings, Edited by M. J. Thompson, P. G. LeComber, Y. Hamakawa ,A. Madan and E. Schiff, 1992, p. 1151.
8. Backscattering Spectrometry, W. K. Chu, J. W. Mayer, and M. A. Nicolet, Academic Press, NY, 1978.
9. L. R. Doolittle, Nucl. Inst. Meth. **B15**, 1986, 227.
10. B. E. Anspaugh and R. G. Downing, 17st IEEE Photovoltaic Specialists Conference Proceedings, 1984, p. 23.
11. H. Dursch, W. Chen and D. Russel, Proc. of the Space Photovoltaic Research and Technology Conference, NASA Conference Publication 2408, 1985, p. 165.
12. J.J. Hanak, A. Myatt, P. Nath and J.R. Woodyard, Proc. of the 18th IEEE Photovoltaic Specialists Conference, 1985, p. 1718.
13. I. Weinberg, C.K. Swartz and R.E. Hart Jr., Proc. of the 20th IEEE Photovoltaic Specialist Conference, 1988, p.893.